Atmos. Meas. Tech., 5, 2593–2600, 2012
www.atmos-meas-tech.net/5/2593/2012/
doi:10.5194/amt-5-2593-2012

Atmospheric Measurement Techniques

Usability of optical spectrum analyzer in measuring atmospheric CO_2 and CH_4 column densities: inspection with FTS and aircraft profiles in situ

M. Kawasaki[1,2], H. Yoshioka[2], N. B. Jones[3], R. Macatangay[3], D. W. T. Griffith[3], S. Kawakami[4], H. Ohyama[4], T. Tanaka[4], I. Morino[5], O. Uchino[5], and T. Ibuki[2]

[1]Research Institute for Humanity and Nature, Kyoto 603-8047, Japan
[2]Department of Molecular Engineering, Kyoto University, Kyoto 615-8510, Japan
[3]School of Chemistry, Northfields Ave, University of Wollongong, NSW 2522, Australia
[4]Japan Aerospace Exploration Agency, Tsukuba, Ibaraki 305-8505, Japan
[5]National Institute for Environmental Studies, Tsukuba, Ibaraki 305-8506, Japan

Correspondence to: T. Ibuki (ibuki-90123@maia.eonet.ne.jp)

Received: 16 May 2012 – Published in Atmos. Meas. Tech. Discuss.: 12 June 2012
Revised: 24 September 2012 – Accepted: 8 October 2012 – Published: 1 November 2012

Abstract. The practical usefulness of a desktop optical spectrum analyzer (OSA) for measuring atmospheric CO_2 and CH_4 column densities at surface sites was examined in two separate measurement campaigns. The first comparison involved operating the OSA in parallel with a high resolution Fourier transform spectroscopy (FTS) situated at the University of Wollongong in Australia. Scale factors for the OSA were assigned for the column average volume mixing ratios of $x$$CO_2$ and $x$$CH_4$ by comparing with the well-studied FTS. The second method is a calibration against aircraft CO_2 profiles in situ over Tsukuba in Japan obtained during a GOSAT validation campaign carried out from 28 January to 7 February 2011. The $x$$CO_2$ values in the campaign, deduced by use of a derived OSA scale factor, were in excellent agreement with the integrated aircraft profiles.

1 Introduction

Carbon dioxide and methane have the highest and the second highest contributions of ~ 64 and ~ 18 %, respectively, to overall global radiative forcing from major anthropogenic greenhouse gases (WMO, 2011). The growth rate of atmospheric CO_2 averaged 2.9 PgC yr^{-1} or 1.37 ppm yr^{-1} in 1959–2006 (Canadell et al., 2007) and has increased to the annual mean growth rate of 2.38 ppm yr^{-1} in 2010 (NOAA). The concentration of CO_2 in the marine surface layer has increased by 50 ppm in the last 30 yr (NOAA), and the global temperature has increased by about 0.6 °C (Brohan et al., 2006). Estimation of source and sink strengths is required to better manage CO_2 gas emission. The Greenhouse gases Observing Satellite (GOSAT: IBUKI) of Japan was launched on 23 January 2009, and data acquisition for the CO_2 and CH_4 column densities has progressed by using an onboard Fourier transform spectrometer, FTS (Kuze et al., 2009), with good precision from space. The Total Carbon Column Observing Network (TCCON: http://www.tccon.caltech.edu) is a network of ground-based FTS instruments with high-resolution providing precise column densities of CO_2, O_2, CH_4, H_2O, HDO, HF, CO, N_2O, etc. (Wunch et al., 2011). TCCON is composed of 21 sites at this moment in time, and 15 FTS instruments are operational in Canada, USA, New Zealand, Australia, Japan and some European countries. The TCCON data are highly reliable and are used for validations of GOSAT and other satellites (Washenfelder et al., 2006; Deutscher et al., 2010; Wunch et al., 2010; Morino et al., 2011). However, surface monitoring sites of total column densities of greenhouse gases are lacking in many developing countries in the Asian, African and South American continents and on oceans. One of the reasons for this is probably due to the high setup cost of an FTS. In addition most existing FTS instruments are located in an air-conditioned room.

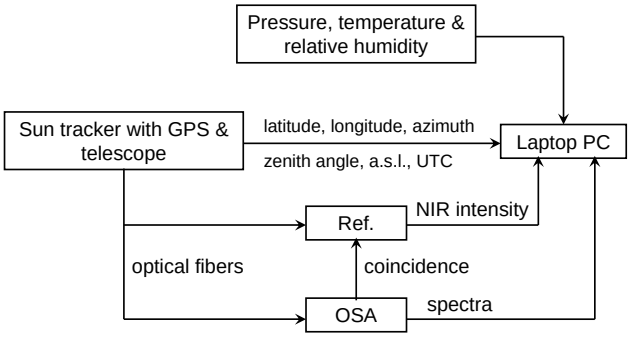

Fig. 1. Block diagram of the data acquisition system.

An automated FTS housed in a 20-foot shipping container has been developed for remote measurement (Geibel et al., 2010). This system is transportable by truck, train or ship but is still large and heavy.

In a previous paper we have proposed a desktop optical spectrum analyzer (OSA) for measuring atmospheric CO_2 and CH_4 column densities at surface monitoring sites (Kobayashi et al., 2010: hereafter denoted as Part 1). The grating-based OSA resolves rotational lines of CO_2 and CH_4 in the near infrared (NIR) region. The OSA instrument is compact, portable, low cost, rugged and basically maintenance free.

In the present paper the practical usefulness of the OSA system was examined for measuring atmospheric CO_2 and CH_4 column densities using two methods: one of them is a parallel measurement with a TCCON FTS at the University of Wollongong (UoW) for 14 months, in which scale factors for the column averaged volume mixing ratios of xCO_2 and xCH_4 were determined. The second method uses aircraft CO_2 profiles obtained in a GOSAT validation carried out at Tsukuba in Japan, a TCCON site, on 28 January–7 February 2011, which provided the opportunity to compare the scale factor against the aircraft profiles measured in situ. In this campaign the xCO_2 and xCH_4 from the OSA were also compared with those obtained with the FTS operated by the Japan Aerospace Exploration Agency (JAXA) measured under the same conditions.

2 Instrumental

The system for measuring atmospheric CO_2 and CH_4 column densities is composed of a desktop OSA (Yokogawa AQ6370 series) and a portable sun tracker as described in detail in Part 1. A block diagram of the data acquisition is shown in Fig. 1. The OSA (AQ6370-custom) disperses radiation from 600 to 1800 nm, and its dimensions are 43(W) × 22(H) × 46(D) cm with a weight of 19 kg. The wavelength resolution is 0.08 cm^{-1} at 1600 nm (6250 cm^{-1}), but this depends on the core size of optical fibre employed. The OSA wavelength is self-calibrated by an internal C_2H_2 gas cell. The portable sun tracker was equipped with a GPS and a small telescope for concentrating the sunlight onto an optical fibre. A long-pass filter (HOYA RM100, $\lambda >$ 1000 nm) was attached at the front of the object lens of the telescope to cut off the second-order stray light. Geophysical data of latitude, longitude, a.s.l. and UTC from the GPS and meteorological information of pressure, temperature and relative humidity on the measuring surface site are accumulated through a data logger on a laptop computer. The pressure on the surface was monitored by a pressure transducer (Setra 276: Part 1) with a stated accuracy of ±0.25 % FS. The pressure measurement was compared against a precision aneroid barograph (with an accuracy of ±0.7 hPa and the minimum readout of 0.5 hPa, Ota Keiki Seisakusho Co., 9-A-05) and agreed within ±2 hPa at 1000 hPa. Solar absorption spectra measured by the OSA were stored in the laptop computer. Reference solar intensity in the region of 1000–1700 nm monitored by an InGaAs detector was coincidently measured with the spectrum signal and used to compensate for fluctuations in the sunlight intensity. The whole system is automated and requires electric power of 100–240 VAC with a maximum 450 VA and a flat space of 70 × 70 cm^2 for each OSA and associated sun tracker. The system is able to be transported in a car and set up by a single person within a day.

3 Performances for practical usability of the OSA

3.1 OSA measurements in parallel with FTS

Solar absorption spectra in the regions of 1569–1575 and 1673–1679 nm were measured for the CO_2 and CH_4 rotational lines, respectively, from July 2010 to August 2011 at UoW in Australia. Typical spectra from the OSA are shown in Fig. 2 where the black and red curves are the observed and fitted spectra, respectively. The residual is shown in the top panel. The full widths at half maximum of the peaks were found to be 0.2090 and 0.1475 cm^{-1} for CO_2 and CH_4, respectively, deduced as a fitting parameter under standard operational conditions of the OSA. The absorption spectra of CO_2 and CH_4 were also measured by a Bruker IFS 125HR FTS under the same conditions following TCCON standards. The OSA and FTS systems were operated in parallel about 2 m apart fed by their respective solar beams under the same weather conditions. The spectra obtained by the FTS and the OSA were independently retrieved, respectively, by means of the GFIT algorithm (Version 4.4.2: Toon et al., 1992; Wunch et al., 2011) and the software given in Part 1 where a constant volume mixing is assumed and the HITRAN 2008 database (Rothman et al., 2009) is adopted.

3.1.1 Carbon dioxide

The column average volume mixing ratio xCO_2 is defined as the ratio of the column density of CO_2 to the total column of

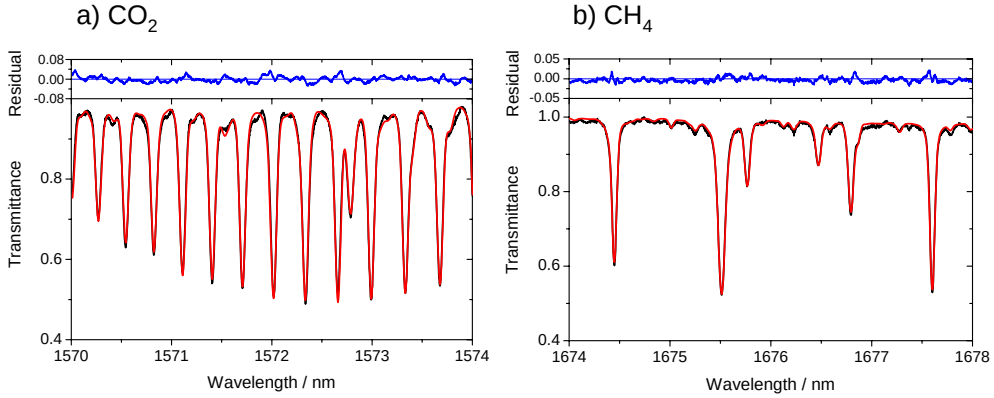

Fig. 2. Absorption spectra of CO_2 and CH_4. Black and red curves denote the observed and fitted spectra, respectively. The residual is shown in the top panel.

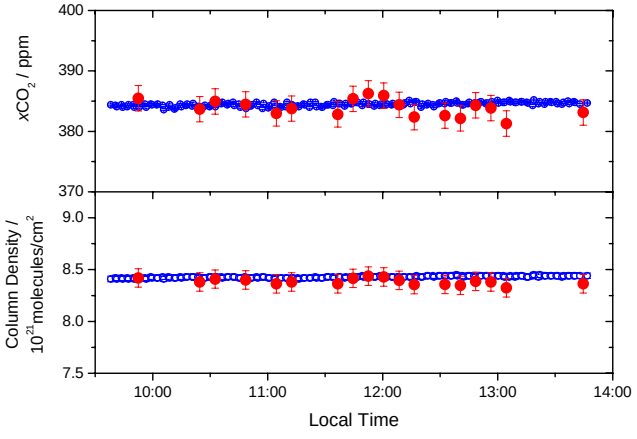

Fig. 3. Time series of column density and $x\mathrm{CO}_2$ on 3 July 2010 at UoW in Australia. OSA: solid circles (scale factor for $x\mathrm{CO}_2$: SF = 1.008); FTS: open circles with estimated errors (SF = 0.989).

dry air (Washenfelder et al., 2006):

$$x\mathrm{CO}_2 = [\text{column of } \mathrm{CO}_2]/[\text{total column of dry air}] \quad (1)$$

where the total column of dry air is given by

$$[\text{total column of dry air}] = [\text{total column of air}] - [\text{column of } \mathrm{H_2O}]. \quad (2)$$

The total column of air is calculated by use of the pressure measured at the surface site, the gravitational acceleration, the molecular weight of air and Avogadro's constant. The profiles of temperature, pressure and relative humidity against altitude are available from the database of National Centers for Environmental Prediction/National Center for Atmospheric Research (NCEP/NCAR, 2010–2011) to calculate the column of H_2O.

An example of daily analyses is shown in Fig. 3 for 3 July 2010 where the solid and the open circles represent the OSA and the UoW FTS measurements, respectively. In the present OSA analyses, a discrimination level of 3 % was employed for the fractional solar variation monitored as the NIR intensity shown in Fig. 1. The scale factor for $x\mathrm{CO}_2$ from the OSA is given just below. In spite of several times larger standard deviations of the OSA in the third and sixth columns in Table 1, the averages of the column density and $x\mathrm{CO}_2$ from the OSA (the second and fifth columns) are very close to those from the FTS. Sources of the errors for the TCCON FTS measurements have been described in detail (Wunch et al., 2011). The standard deviation of the OSA measurements for the 132 days from July 2010 to September 2011 was assigned to the uncertainty of the present system.

Time series of 14 months of the column density and $x\mathrm{CO}_2$ for the OSA are shown in Fig. 4 where scaled data from the FTS are superimposed over the period July–October 2010 for the column density and July 2010–June 2011 for $x\mathrm{CO}_2$. The averages between 10:00–14:00 LT, while the solar intensity is stable, were plotted with the standard deviations. Averages of the OSA and FTS column densities measured during July–October were $(8.369 \pm 0.087) \times 10^{21}$ and $(8.413 \pm 0.056) \times 10^{21}$ molecules cm^{-2}, respectively, a ratio of 0.995 and thus in good agreement. The straight line in the upper panel has a slope of the global CO_2 growth rate of 2.38 ppm yr^{-1} in 2010 (NOAA).

The scale factor of 0.989 has been applied to the $x\mathrm{CO}_2$ from the FTS instruments in the TCCON network derived from aircraft profiles measured over the TCCON sites in order to place them on the World Meteorological Organization (WMO) standard reference scales (Wunch et al., 2010). The CO_2 scale factors for the present OSA are given in the fifth column in Table 2: they were determined to be the ratio of the mean CO_2 concentration over two months (the third column) derived by the fitting algorithm described in Part 1 relative to $x\mathrm{CO}_2$ in the same period from the FTS (the fourth column). The average of 1.008 ± 0.002 was assigned to the scale factor for $x\mathrm{CO}_2$ from the OSA. The standard deviations in the $x\mathrm{CO}_2$ from the OSA are less than ± 0.6 % (the third column) but still larger than those from the FTS (the fourth column)

Table 1. Column densities and $x\mathrm{CO_2}$ from the OSA and FTS on 3 July 2010 at the University of Wollongong Australia.

Instrument	Column density[a]	Standard deviation	Uncertainty estimated	$x\mathrm{CO_2}$ ppm	Standard deviation	Uncertainty estimated
OSA	8.384	0.031	0.09[b]	383.88	1.39	2.1[b]
FTS (UoW)	8.429	0.009	0.10	384.48	0.32	1.0

[a] Units in 10^{21} molecules cm^{-2}. [b] Standard deviation of the OSA measurements July 2010–September 2011.

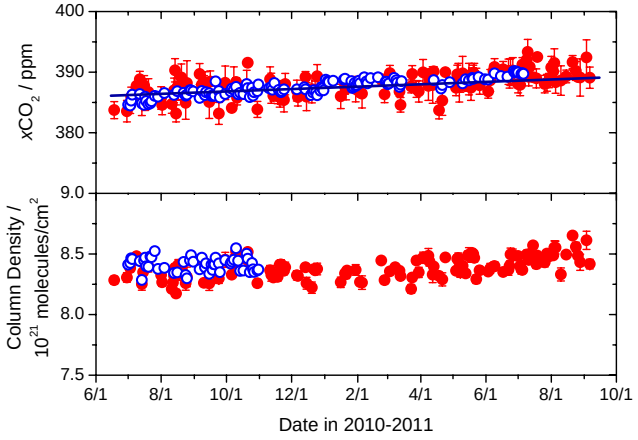

Fig. 4. Time series of column density and $x\mathrm{CO_2}$ with the standard deviations for 14 months at UoW in Australia. OSA: solid circles (SF = 1.008); FTS: open circles (SF = 0.989). The line in the top panel has a slope of the global growth rate 2.38 ppm yr^{-1} in 2010.

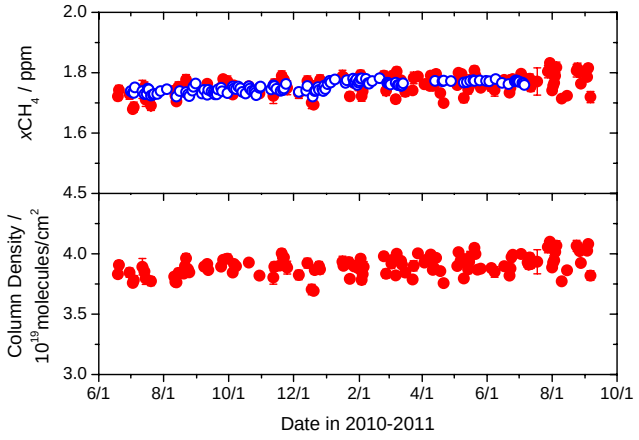

Fig. 5. Time series of column density and $x\mathrm{CH_4}$ with the standard deviations for 14 months at UoW in Australia. OSA: solid circles (SF = 1.035); FTS: open circles (SF = 0.978).

by 2–4 times. The numerals in the last column indicate the total number of days used in evaluating the scale factors.

3.1.2 Methane

A typical spectrum of methane along with a model fit and difference obtained with the OSA is shown in Fig. 2b. The two peaks at 1674.4 and 1677.6 nm have been assigned to the absorption of $\mathrm{CH_4}$ while the other features are water or Fraunhofer lines. The scale factor of 1.035 ± 0.004 for $x\mathrm{CH_4}$ in Table 2 was obtained as an adjusting parameter between the OSA and FTS $x\mathrm{CH_4}$ normalized by the TCCON scale factor of 0.978 (Wunch et al., 2010). The standard deviations in the mean $x\mathrm{CH_4}$ from the OSA (the sixth column in Table 2) are similarly larger to the case of $x\mathrm{CO_2}$.

Time series of the column density and $x\mathrm{CH_4}$ are shown in Fig. 5 where the solid and the open circles are from the OSA and FTS, respectively. The averages of the column density and $x\mathrm{CH_4}$ from the OSA over a period of 14 months were $(3.886 \pm 0.071) \times 10^{19}$ molecules cm^{-2} and 1.759 ± 0.030 ppm, respectively. The latter agrees with the value of 1.766 ± 0.008 ppm at Baring Head in New Zealand (41.41° S, 174.87° E) measured by means of gas chromatography from June to December 2010 (WMO WDCGG). The seasonal cycle observed in the flask samplings at Baring Head, however, was not clear in the OSA data as it may be buried in the measurement noise.

3.2 Inspection with GOSAT validation campaign

The OSA was compared with GOSAT measurements in a validation campaign that took place at Tsukuba Japan in collaboration with JAXA and the National Institute for Environmental Studies of Japan on 28, 31 January, 3 and 7 February 2011 by flying an aircraft (Beechcraft King Air 200T: Tanaka et al., 2012) over Tsukuba. The colocation of the aircraft spiral flights with respect to the OSA was less than 15 km. The aircraft carried onboard continuous $\mathrm{CO_2}$ measuring equipment (CME) with an accuracy of ± 0.2 ppm (Machida et al., 2008; Tanaka et al., 2012). The lowest and highest sampling points from the aircraft were 390 m and 7 km in altitude, respectively. Meteorological data were obtained from the surface up to 20 km for pressure, temperature, relative humidity, wind direction and wind speed by launching GPS radiosondes (Meisei Electric Co. RS-01G: accuracy ± 0.5 °C, ± 7 % RH). The flight time of the aircraft overlapped with the duration of the radiosonde.

We examined the $x\mathrm{CO_2}$ mixing ratio from an OSA by comparing with two measurements: in situ aircraft profiles of $\mathrm{CO_2}$ and a ground-based Bruker IFS 125HR FTS housed in a shipping container which participated in the campaign. The

Table 2. Scale factors for $x\mathrm{CO_2}$ and $x\mathrm{CH_4}$ from the OSA.

Year	Month	Mean $x\mathrm{CO_2}$ in 2 months		SF[a]	Mean $x\mathrm{CH_4}$ in 2 months		SF	Total
		OSA[b]	FTS (UoW)	$\mathrm{CO_2}$	OSA	FTS (UoW)	$\mathrm{CH_4}$	days
2010	July–August	389.67 ± 1.82	385.83 ± 0.85	1.010	1.792 ± 0.030	1.737 ± 0.011	1.032	20
	September–October	390.31 ± 2.35	386.77 ± 0.70	1.009	1.812 ± 0.017	1.741 ± 0.009	1.041	15
	November–December	390.11 ± 1.17	387.04 ± 0.47	1.008	1.814 ± 0.029	1.745 ± 0.009	1.039	18
2011	January–February	390.22 ± 2.71	388.41 ± 0.47	1.005	1.825 ± 0.024	1.772 ± 0.007	1.030	12
	March–April	390.90 ± 2.01	388.20 ± 0.50	1.007	1.824 ± 0.030	1.765 ± 0.006	1.033	16
	May–June	392.19 ± 1.09	389.26 ± 0.61	1.007	1.827 ± 0.020	1.772 ± 0.004	1.031	21

[a] SF denotes scale factor. Average = 1.008 ± 0.002 and 1.035 ± 0.004 for $x\mathrm{CO_2}$ and $x\mathrm{CH_4}$, respectively. [b] Units in ppm.

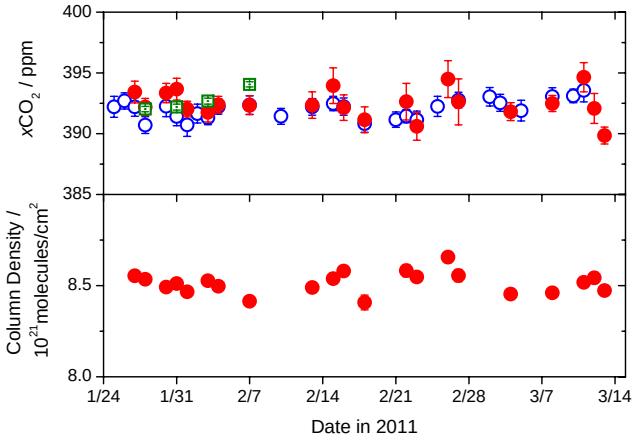

Fig. 6. Time series of column density and $x\mathrm{CO_2}$ with the standard deviations at JAXA in Tsukuba, Japan. OSA: solid circles (SF = 1.008); FTS: open circles (SF = 0.989); Aircraft: open squares.

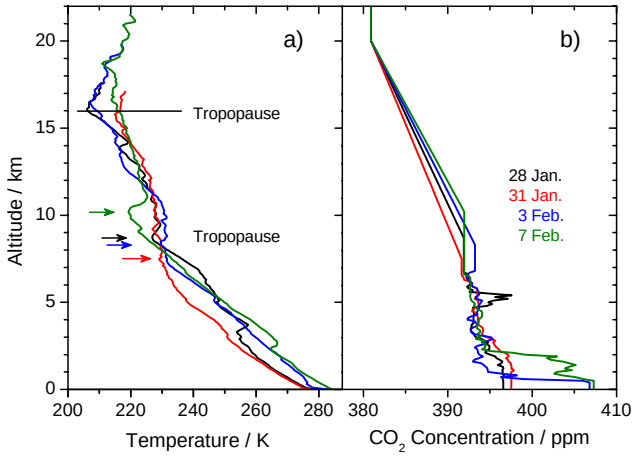

Fig. 7. Vertical profiles of temperature and $\mathrm{CO_2}$ concentration over Tsukuba in Japan on 28 (black), 31 January (red), 3 (blue) and 7 February 2011 (olive). Details are given in the text.

FTS was operated by JAXA, and the spectra were retrieved using the GFIT algorithm. The $x\mathrm{CH_4}$ mixing ratio from the OSA was checked against the JAXA FTS. The sun tracker feeding the solar beam to the OSA was located on the roof of the shipping container about 2 m apart from the sunlight inlet of the JAXA FTS in order to obtain spectra recorded under the same weather conditions. The OSA and FTS were operated from 25 January to 13 March in 2011.

3.2.1 Carbon dioxide

Figure 6 shows the results obtained by the OSA (solid circles), the JAXA FTS (open circles) and the aircraft (open squares), where the scale factor for the OSA as determined in Sect. 3.1.1 was employed. The average $x\mathrm{CO_2}$ from the OSA and FTS over the 7 weeks were 392.74 ± 1.18 and 391.85 ± 0.79 ppm, respectively, in agreement with a ratio of 0.998. The weather in the latter half of February was cloudy and probably contributed to the large standard deviation in the OSA data. The maximum and minimum differences in the $x\mathrm{CO_2}$ between the OSA and FTS were 2.45 ppm on 31 January and −0.51 ppm on 8 March, respectively. The average $x\mathrm{CO_2}$ from the OSA at UoW during 31 January–13 March was 387.23 ± 1.57 ppm, being lower than that at JAXA in Tsukuba by 5.5 ppm.

The vertical profiles of temperature over Tsukuba measured by the sondes are shown in Fig. 7a where the first tropopauses lie at 8.7, 7.5, 8.3 and 10.2 km on 28 January (black), 31 January (red), 3 February (blue) and 7 February (olive), respectively, indicated by arrows while a common second tropopause exists around 16 km. Tropospheric $\mathrm{CO_2}$ concentrations were measured in situ by means of the CME installed in the aircraft with a height profile ranging from about 400 m to 7 km in altitude. The vertical $\mathrm{CO_2}$ profiles over Tsukuba were depicted by a previously reported estimation (Araki et al., 2010): the $\mathrm{CO_2}$ concentration at the lowest observable point was assumed to continue down to the surface while that at the highest point at about 7 km extends up to the first tropopause (Fig. 7b). The $\mathrm{CO_2}$ concentration at the first tropopause was assumed to decrease linearly to the value at 20 km in altitude (Araki et al., 2010).

Table 3. Volume mixing ratios by aircraft, OSA and FTS at Tsukuba in Japan.

Date in 2011	Aircraft[a]	OSA	Ratio[b]	FTS (JAXA)	Ratio
28 January	392.03 ± 0.22	392.19 ± 0.71	1.000	390.53 ± 0.68	0.996
31 January	392.19 ± 0.25	393.67 ± 0.89	1.004	391.22 ± 0.77	0.998
3 February	392.68 ± 0.24	391.76 ± 0.79	0.998	391.12 ± 0.58	0.996
7 February	394.05 ± 0.21	392.34 ± 0.77	0.996	392.17 ± 0.77	0.995

[a] Units in ppm. [b] Ratio denotes the relative $x\mathrm{CO_2}$ from the OSA or FTS (JAXA) to that from the aircraft. Average = 0.999 ± 0.003 and 0.996 ± 0.001 for OSA and FTS (JAXA), respectively.

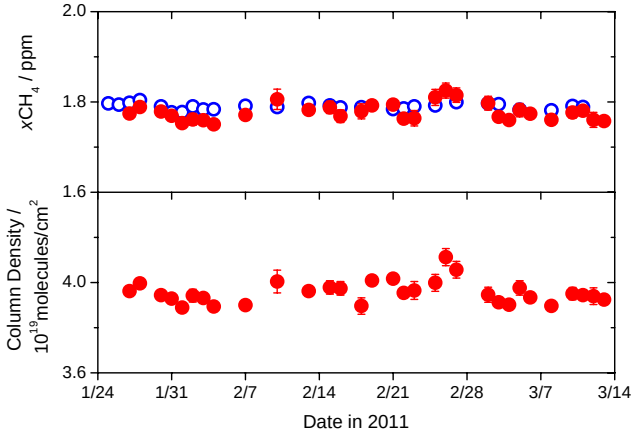

Fig. 8. Time series of column density and $x\mathrm{CH_4}$ with the standard deviations at JAXA in Tsukuba, Japan. OSA: solid circles (SF = 1.035); FTS: open circles (SF = 0.978).

The stratospheric $\mathrm{CO_2}$ concentration above 20 km is considered to be constant, the value of which lags about five years behind the global mean $\mathrm{CO_2}$ in the troposphere (Aoki et al., 2003). Thus the annual mean $\mathrm{CO_2}$ of 380.91 ppm in 2006 (NOAA) was adopted in the present work as the concentration above 20 km in altitude.

Table 3 summarizes the integrated aircraft $x\mathrm{CO_2}$, OSA and FTS for the 4 days of the comparison. The aircraft $x\mathrm{CO_2}$ derived from the vertical profile mentioned above is given in the second column. Contributing uncertainties to the total aircraft $x\mathrm{CO_2}$ were assumed to be 1.76, 1.58, 1.58, and 0.2 ppm for the stratospheric extrapolation above 20 km in altitude, missing tropospheric values for the 4 days, usage of contemporary profile between the highest measurement point and the first tropopause, and mean aircraft profile, respectively (Messerschmidt et al., 2011). The annual growth rate of 1.76 ppm in 2006 (NOAA) was assumed to be the uncertainty above 20 km. The largest difference of 1.58 ppm at the highest points observed in the 4 days was assigned to both the missing tropospheric values and usage of a contemporary profile. The CME installed in the aircraft has an overall precision of 0.2 ppm (Machida et al., 2008; Tanaka et al., 2012). The total uncertainty of the aircraft in situ was thus estimated as the sum in quadrature after weighting by pressure.

The volume mixing ratios from the OSA and FTS relative to that from the aircraft (the fourth and last columns) give the averages of 0.999 ± 0.003 and 0.996 ± 0.001, respectively, indicating that the three independent measurements are in good agreement. This also shows that the scale factor of 1.008 for the OSA deduced in Sect. 3.1.1 is consistent with both FTS and aircraft results. The difference in $x\mathrm{CO_2}$ between the aircraft and the OSA or FTS on 7 February is larger than usual, -1.7 or -1.9 ppm, respectively. The reason for the deviation is not clear, but the NIR intensity reference signal (Fig. 1) was 10 % weaker than the other 3 days, most likely due to the presence of thin clouds and this may therefore result in the less reliable value for $x\mathrm{CO_2}$.

3.2.2 Methane

Time series of $x\mathrm{CH_4}$ and column densities for methane at Tsukuba Japan are depicted in Fig. 8. The $x\mathrm{CH_4}$ from the OSA is examined with parallel measurement from the JAXA FTS: the averages of $x\mathrm{CH_4}$ from the OSA (solid circles) and FTS (open circles) were 1.778 ± 0.019 and 1.790 ± 0.007 ppm, respectively, for the 7 weeks, which are in good agreement. The mean $x\mathrm{CH_4}$ at UoW in the same period was 1.764 ± 0.026 ppm, being lower than those at JAXA in Tsukuba by 14–26 ppb. Concentrations of $\mathrm{CH_4}$ in the air analyzed by precision instruments are lower in the Southern Hemisphere than in the Northern Hemisphere (WMO, 2006), and thus the present observation of $x\mathrm{CH_4}$ is consistent with the global trend of $\mathrm{CH_4}$. However, when we take into account the standard deviations in $x\mathrm{CH_4}$, the present difference is only qualitative. The mean column density was $(3.948 \pm 0.048) \times 10^{19}$ molecules $\mathrm{cm^{-2}}$ at JAXA while that at UoW during this period was $(3.899 \pm 0.060) \times 10^{19}$ molecules $\mathrm{cm^{-2}}$, being a little low but still within the measurement noise.

4 Summary

Two field campaigns presented in this paper have shown that an optical spectrum analyzer (OSA) is a promising technology for measuring atmospheric $\mathrm{CO_2}$ and $\mathrm{CH_4}$ column densities at surface sites. The OSA, due to its smaller physical size and lower cost, is expected to provide a supplemental

measuring system to the existing FTS network. The standard deviation of the retrieved OSA column density at present is 2–4 times higher than that of the collocated FTS. The data quality will be improved in future through improvements in the analysis procedures, the shortening of the data acquisition intervals and the application of more stringent data quality criteria.

Acknowledgements. The authors are grateful to Chris Brion of University of British Columbia in Canada for comments, the National Institute of Water & Atmospheric Research Ltd. for providing the CH_4 concentration data at Baring Head in New Zealand, the Yokogawa Meter & Instruments Co. Ltd. for renting the optical spectrum analyzer for a long term, and the GRENE project from Ministry of Education, Science, Culture and Sports of Japan for partial financial support. The NCEP data for this study are from the Research Data Archive (RDA) which is maintained by the Computational and Information Systems Laboratory (CISL) at the National Center for Atmospheric Research (NCAR). NCAR is sponsored by the National Science Foundation (NSF). The original data are available from the RDA (http://dss.ucar.edu) in dataset number ds083.2.

Edited by: J. Notholt

References

Aoki, S., Nakazawa, T., Machida, T., Sugawara, S., Morimoto, S., Hashida, G., Yamanouchi, T., Kawamura, K., and Honda, H.: Carbon dioxide variations in the stratosphere over Japan, Scandinavia and Antarctica, Tellus, 55B, 178–186, doi:10.1034/j.1600-0889.2003.00059.x, 2003.

Araki, M., Morino, I., Machida, T., Sawa, Y., Matsueda, H., Ohyama, H., Yokota, T., and Uchino, O.: CO_2 column-averaged volume mixing ratio derived over Tsukuba from measurements by commercial airlines, Atmos. Chem. Phys., 10, 7659–7667, doi:10.5194/acp-10-7659-2010, 2010.

Brohan, P., Kennedy, J. J., Harris, I., Tett, S. F. B., and Jones, P. D.: Uncertainty estimates in regional and global observed temperature changes: a new dataset from 1850, J. Geophys. Res., 111, D12106, doi:10.1029/2005JD006548, 2006.

Canadell, J. G., Le Quéré, C., Raupach, M. R., Field, C. B., Buitenhuis, E. T., Ciais, P., Conway, T. J., Gillett, N. P., Houghton, R. A., and Marland, G.: Contributions to accelerating atmospheric CO_2 growth from economic activity, carbon intensity, and efficiency of natural sinks, Proc. Natl. Acad. Sci. USA, 104, 18866–18870, doi:10.1073/pnas.0702737104, 2007.

Deutscher, N. M., Griffith, D. W. T., Bryant, G. W., Wennberg, P. O., Toon, G. C., Washenfelder, R. A., Keppel-Aleks, G., Wunch, D., Yavin, Y., Allen, N. T., Blavier, J.-F., Jiménez, R., Daube, B. C., Bright, A. V., Matross, D. M., Wofsy, S. C., and Park, S.: Total column CO_2 measurements at Darwin, Australia – site description and calibration against in situ aircraft profiles, Atmos. Meas. Tech., 3, 947–958, doi:10.5194/amt-3-947-2010, 2010.

Geibel, M. C., Gerbig, C., and Feist, D. G.: A new fully automated FTIR system for total column measurements of greenhouse gases, Atmos. Meas. Tech., 3, 1363–1375, doi:10.5194/amt-3-1363-2010, 2010.

Kobayashi, N., Inoue, G., Kawasaki, M., Yoshioka, H., Minomura, M., Murata, I., Nagahama, T., Matsumi, Y., Tanaka, T., Morino, I., and Ibuki, T.: Remotely operable compact instruments for measuring atmospheric CO_2 and CH_4 column densities at surface monitoring sites, Atmos. Meas. Tech., 3, 1103–1112, doi:10.5194/amt-3-1103-2010, 2010.

Kuze, A., Suto, H., Nakajima, M., and Hamazaki, T.: Thermal and infrared sensor for carbon observation Fourier-transform spectrometer on the Greenhouse Gases Observing Satellite for greenhouse gases monitoring, Appl. Optic., 48, 6716–6733, doi:10.1364/AO.48.006716, 2009.

Machida, T., Matsueda, H., Sawa, Y., Nakagawa, Y., Hirotani, K., Kondo, N., Goto, K., Nakazawa, T., Ishikawa, K., and Ogawa, T.: Worldwide measurements of atmospheric CO_2 and other trace gas species using commercial airlines, J. Atmos. Ocean. Tech., 25, 1744–1754, doi:10.1175/2008JTECHA1082.1, 2008.

Messerschmidt, J., Geibel, M. C., Blumenstock, T., Chen, H., Deutscher, N. M., Engel, A., Feist, D. G., Gerbig, C., Gisi, M., Hase, F., Katrynski, K., Kolle, O., Lavrič, J. V., Notholt, J., Palm, M., Ramonet, M., Rettinger, M., Schmidt, M., Sussmann, R., Toon, G. C., Truong, F., Warneke, T., Wennberg, P. O., Wunch, D., and Xueref-Remy, I.: Calibration of TCCON column-averaged CO_2: the first aircraft campaign over European TCCON sites, Atmos. Chem. Phys., 11, 10765–10777, doi:10.5194/acp-11-10765-2011, 2011.

Morino, I., Uchino, O., Inoue, M., Yoshida, Y., Yokota, T., Wennberg, P. O., Toon, G. C., Wunch, D., Roehl, C. M., Notholt, J., Warneke, T., Messerschmidt, J., Griffith, D. W. T., Deutscher, N. M., Sherlock, V., Connor, B., Robinson, J., Sussmann, R., and Rettinger, M.: Preliminary validation of column-averaged volume mixing ratios of carbon dioxide and methane retrieved from GOSAT short-wavelength infrared spectra, Atmos. Meas. Tech., 4, 1061–1076, doi:10.5194/amt-4-1061-2011, 2011.

NCAR: National Center for Atmospheric Research, available at: http://dss.ucar.edu/datasets/ds083.2/ (last access: September 2011), 2011.

NOAA: Earth System Research Laboratory, available at: http://www.esrl.noaa.gov/gmd/ccgg/trends/global.html (last access: December 2011), 2011.

Rothman, L. S., Gordon, I. E., Barbe, A., Benner, D. C., Bernath, P. F., Birk, M., Boudon, V., Brown, L. R., Campargue, A., Champion, J.-P., Chance, K., Coudert, L. H., Dana, V., Devi, V. M., Fally, S., Flaud, J.-M. Gamache, R. R., Goldman, A., Jacquemart, D., Kleiner, I., Lacome, N., Lafferty, W. J., Mandin, J.-Y., Massie, S. T., Mikhailenko, S. N., Miller, C. E., Moazzen-Ahmadi, N., Naumenko, O. V., Nikitin, A. V., Orphal, J., Perevalov, V. I., Perrin, A., Predoi-Cross, A., Rinsland, C. P., Rotger, M., Šimeèková, M., Smith, M. A. H., Sung, K., Tashkun, S. A., Tennyson, J., Toth, R. A., Vandaele, A. C., and Auwera, J. V.: The HITRAN 2008 molecular spectroscopic database, J. Quant. Spectrosc. Ra., 110, 533–572, doi:10.1016/j.jqsrt.2009.02.013, 2009.

Tanaka, T., Miyamoto, Y., Morino, I., Machida, T., Nagahama, T., Sawa, Y., Matsueda, H., Wunch, D., Kawakami, S., and Uchino, O.: Aircraft measurements of carbon dioxide and methane for the calibration of ground-based high-resolution Fourier Transform Spectrometers and a comparison to GOSAT data measured over Tsukuba and Moshiri, Atmos. Meas. Tech., 5, 2003–2012, doi:10.5194/amt-5-2003-2012, 2012.

Toon, G. C., Farmer, C. B., Schaper, P. W., Lowes, L. L., and Norton, R. H.: Composition measurements of the 1989 Arctic winter stratosphere by airborne infrared solar absorption spectroscopy, J. Geophys. Res., 97, 7939–7961, doi:10.1029/91JD03114, 1992.

Washenfelder, R. A., Toon, G. C., Blavier, J.-F., Yang. Z., Allen, N. T., Wennberg, P. O., Vay, S. A., Matross, D. M., and Daube, B. C.: Carbon dioxide column abundances at the Wisconsin Tall Tower site, J. Geophys. Res., 111, D22305, doi:10.1029/2006JD007154, 2006.

WMO: Greenhouse Gas Bulletin No. 2. The State of Greenhouse Gases in the Atmosphere Using Global Observations through 2005, available at: ftp://ftp.wmo.int/Documents/PublicWeb/arep/gaw/ghg-bulletin-en-11-06.pdf (last access: December 2011), 2006.

WMO: Greenhouse Gas Bulletin No.7. The State of Greenhouse Gases in the Atmosphere Based on Global Observations through 2010, available at: http://www.wmo.int/pages/prog/arep/gaw/ghg/documents/GHGbulletin_7_en.pdf (last access: March 2012), 2011.

WMO WDCGG: available at: http://ds.data.jma.go.jp/gmd/wdcgg/ (last access: December 2011), 2011.

Wunch, D., Toon, G. C., Wennberg, P. O., Wofsy, S. C., Stephens, B. B., Fischer, M. L., Uchino, O., Abshire, J. B., Bernath, P., Biraud, S. C., Blavier, J.-F. L., Boone, C., Bowman, K. P., Browell, E. V., Campos, T., Connor, B. J., Daube, B. C., Deutscher, N. M., Diao, M., Elkins, J. W., Gerbig, C., Gottlieb, E., Griffith, D. W. T., Hurst, D. F., Jiménez, R., Keppel-Aleks, G., Kort, E. A., Macatangay, R., Machida, T., Matsueda, H., Moore, F., Morino, I., Park, S., Robinson, J., Roehl, C. M., Sawa, Y., Sherlock, V., Sweeney, C., Tanaka, T., and Zondlo, M. A.: Calibration of the Total Carbon Column Observing Network using aircraft profile data, Atmos. Meas. Tech., 3, 1351–1362, doi:10.5194/amt-3-1351-2010, 2010.

Wunch, D., Toon, G. C., Blavier, J.-F. L., Washenfelder, R. A., Notholt, J., Connor, B. J., Griffith, D. W. T., Sherlock, V., and Wennberg, P. O.: The Total Carbon Column Observing Network, Phil. Trans. R. Soc. A, 369, 2087–2112, doi:10.1098/rsta.2010.0240, 2011.